

Two-dimensional terahertz photonic crystals fabricated by deep reactive ion etching in Si

Nathan Jukam^{a)} and Mark S. Sherwin

Department of Physics, University of California, Santa Barbara, California 93106

(Received 10 December 2002; accepted 30 April 2003)

Two-dimensional terahertz photonic crystals were manufactured from Si using deep reactive ion etching. Arrays of square holes with widths of 80 (100) μm and lattice constants of 100 (125) μm were etched through 500- μm -thick wafers with high resistivity. Stop bands with transmittance $<1\%$ and widths >200 GHz were observed near 1 THz for light with an electric field vector in the plane of the wafers (TE polarization). The observed stop bands are close to TE photonic band gaps predicted by a two-dimensional calculation. © 2003 American Institute of Physics.
[DOI: 10.1063/1.1588375]

Photonic crystals (PCs) have band gaps where light cannot propagate. Introducing defects in PCs can create waveguides and resonant cavities for frequencies in the band gap.¹ These waveguides and cavities can be on the order of a wavelength. There has been much work on fabricating photonic crystals for frequencies below 100 GHz and for infrared and optical frequencies.^{2,3} By comparison, there has been relatively little work on PCs for terahertz frequencies.^{4–12} Recent advances in THz detection and generation are leading to new technologies for imaging, communications, and chemical detection.^{13,14} Filters, waveguides, and cavity resonators based on THz PCs may become important components of emerging THz technology.

In this letter, we report the fabrication of two-dimensional (2D) THz PCs made by deep reactive ion etching (DRIE) in Si. DRIE enables the etching of Si with vertical sidewalls and high aspect ratios.¹⁵ Unlike anisotropic wet etching, DRIE is not limited to crystallographic planes.¹⁶ This will make possible the fabrication of THz PC structures with circular holes and fractional edge dislocations.¹⁷

The PC were made from high-resistivity (8–9 K Ω cm) 500- μm -thick Si wafers. High-resistivity Si is transparent at THz frequencies with an index of refraction of 3.42.¹⁸ Square holes with widths w of 80 (100) μm were etched through the wafer using DRIE (see Fig. 1). The holes were arrayed in a square lattice with a lattice constant a of 100 (125) μm that consisted of 10 by 100 (80) unit cells. The sample size was 8 by 11 mm. THz radiation was coupled into the edge of the sample, which served as a slab waveguide.

The first step in the fabrication was to deposit 4.5 μm of SiO₂ by plasma-enhanced chemical vapor deposition on the Si wafers for use as a hard mask during the DRIE. Next, 250 nm of Ni were evaporated for use as a mask during the etching of the SiO₂ hard mask. The Ni mask was made by contact photolithography and a Ni wet etch. Conventional RIE was used to etch the SiO₂ to produce the hard mask for the DRIE. Afterwards, the Ni was completely removed by immersion in the Ni etchant. The wafers were bonded with resist to a 4-in. SiO₂-coated carrier wafer, and the DRIE was

performed by a Plasma-Therm™ 770-ICP. After the DRIE, the wafers were removed from the carrier wafer with acetone, and the remaining SiO₂ was removed with HF.

Transmission spectra were measured with a Bruker IFS 66vs Fourier transform infrared spectrometer (FTIR). An 8–9 K Ω cm Si wafer was cleaved to the approximate dimensions of the samples and was used as a reference. Light was coupled into the edge of the samples by a 2D Winston concentrator.¹⁹ Another 2D Winston concentrator recollimated light that exited the other edge. A piece of THz absorbing foam was pressed against each side of the sample. This eliminated any path for stray light to travel through both Winston concentrators without traveling through the sample. Parabolic $f/4.5$ mirrors were used to focus and collect the light from the Winston concentrators. A wire grid polarizer was placed between the exiting Winston concentrator and the nearest mirror in the FTIR to distinguish between the TE and TM modes. A cold low-pass filter with a 3-dB cutoff of 60 cm^{-1} was placed in front of a composite Si bolometer detector.

Figure 2 shows spectra of power transmitted through the reference and the $a=100$ - μm sample for TE and TM polarizations. The general shape of the spectra represents a convolution of the intensity spectra emitted by the FTIR source with the transmittance of the samples, the beam splitter, and

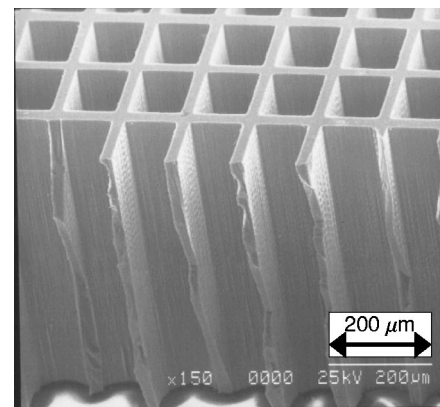


FIG. 1. Scanning electron microscope picture of a PC with $a=125$ μm and $w=100$ μm . The PC cannot be cleaved because of the holes through the wafer. It must be broken, hence the jagged sidewalls.

^{a)}Electronic mail: njukam@physics.ucsb.edu

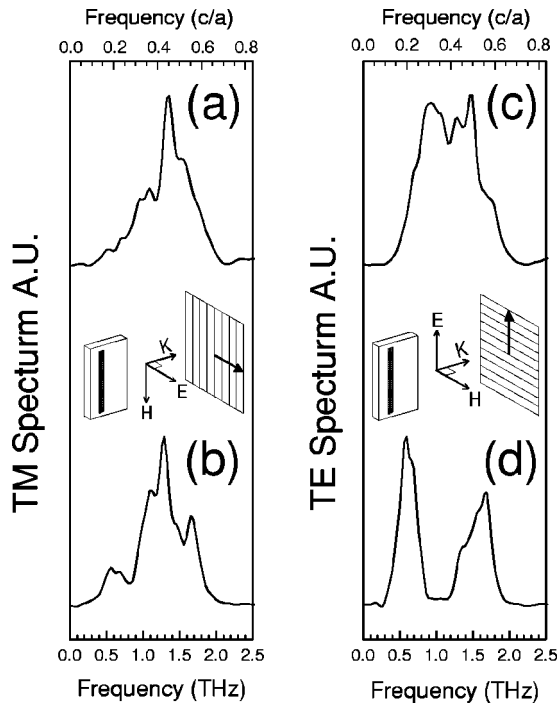


FIG. 2. Power transmitted through reference wafer (a) and (c), and PC (b) and (d), for light polarized in the TM (a) and (b) and TE (c) and (d) directions. The PC had period $a=100\ \mu\text{m}$ and square edge $w=80\ \mu\text{m}$. Insets show sample, light polarization, and wire grid polarizer. All of the figures have been rescaled for visual clarity.

filters. A small dip in the TM spectrum [Fig. 2(b)] is observed at 0.83 THz that is not present in the TM reference spectrum [Fig. 2(a)]. When the polarizer is rotated to select the TE modes, a large stop band in the spectrum of the PC is observed near 1 THz in Fig. 2(d) that is not present in the TE reference spectrum [Fig. 2(c)]. The TE transmittance spectra (sample/reference) of the $a=125\text{-}\mu\text{m}$ and $a=100\text{-}\mu\text{m}$ samples are shown in Fig. 3. A stop band in which the transmittance dips to $<1\%$, is visible for both samples.

The band diagrams of a square 2D lattice with square

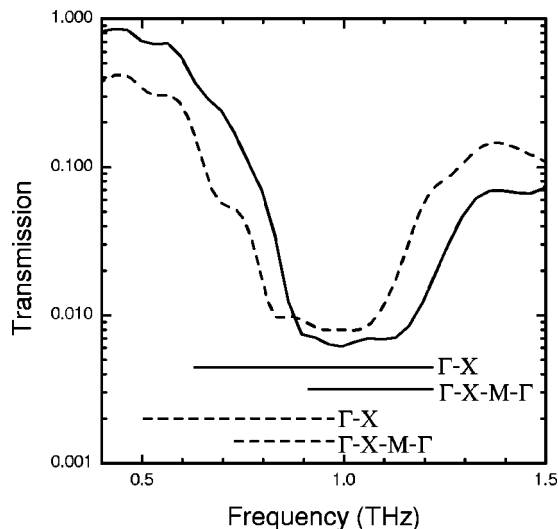


FIG. 3. Transmittance of 2D PCs for TE-polarized light propagating in the Γ -X direction. Solid line (dotted line) is for the crystal with $a=100\ \mu\text{m}$ and $w=80\ \mu\text{m}$ crystal ($a=125\ \mu\text{m}$ and $w=100\ \mu\text{m}$ crystal). The horizontal lines correspond to the calculated 2D TE band gap and the TE band gap in the Γ -X direction.

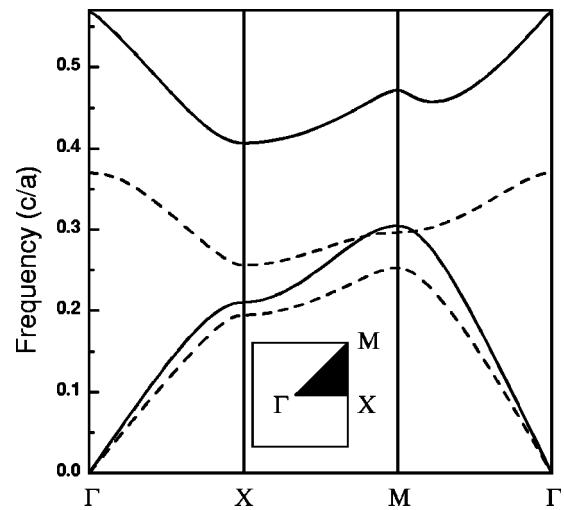


FIG. 4. Photonic band structure for 2D square lattice with $w/a=0.8$. Solid (dashed) lines show first and second TE (TM) bands. The insert shows the irreducible Brillouin zone of a 2D square lattice.

holes and $w/a=0.8$ were computed using the MIT Photonic-BandsTM software.^{20,21} The first and second TE and TM bands of the 2D PC are shown in Fig. 4. The structure has a TE band gap with a width of $0.10\ c/a$, and a very small TM band gap with a width of $0.004\ c/a$. In the Γ -X direction, the direction of propagation for these experiments, the structure has a TE gap extending from $0.21\ c/a$ to $0.41\ c/a$ and a smaller TM gap extending from $0.20\ c/a$ to $0.26\ c/a$. The calculated 2D TE gap in the Γ -X direction and the total TE gap for both samples are shown as lines in Fig. 3 for comparison.

For both samples, the stop bands are close to the predicted values for the total TE gaps. However, the THz radiation propagated mostly in the Γ -X direction. Thus, the stop band is expected to correspond to the Γ -X band gap, which extends to lower frequencies. From the f /number of the beam and the air-Si index mismatch, we estimate the range of angles sampled from the Γ -X direction in the plane of the wafer is 2° .

The dip at .83 THz in the TM spectra in Fig. 2(b) may correspond to the smaller TM gap. Interestingly, this dip is near the lower edge of the TE stop band. This would be expected from Fig. 4, because the Γ -X TM gap is close to the lower Γ -X TE band edge. However, both the TM dip and the lower stop-band edge occur at higher than expected frequencies.

We attribute the discrepancy between the predicted 2D gaps and measured stop bands to two factors. The first, which we believe is the most important, is that the samples were made of $500\text{-}\mu\text{m}$ -thick wafers in order to have sufficient throughput. At THz frequencies, these wafers support several slab waveguide modes that have a component of the wave vector k_z perpendicular to the plane of the waveguide. For a given wave vector k , this will reduce the magnitude of its in-plane component of the wave vector β , where $\beta^2 + k_z^2 = k^2$. This decreases the effective in-plane index of refraction $n_{\text{eff}}=c\beta/\omega$ of the slab mode. It can be shown¹ that for any mode with frequency ω , wave vector k , and index of refraction $n(\mathbf{r})$, if the index is decreased by a factor s such that $n'(\mathbf{r})=n(\mathbf{r})/s$, then the mode with wave vector k is still

a solution to Maxwell's equation, with an *increased* frequency $\omega' = s\omega$. The bands for the higher-order slab modes, which have lower values of n_{eff} , will be shifted up in frequency from the bands of the 2D model. This will increase the lower edge of the stop band. The upper edge of the stop band will not be affected since for lower-order slab modes $k \approx \beta$, and the bands for the higher-order modes all shift upward. Thus, one may expect multimode propagation will increase the stop-band's lower edge, and decrease the stop-band's width. Second, the DRIE was observed to round the corners of the square holes as the etch progressed. Thus, the geometry of the sample is not exactly that of the model.

In conclusion, we have demonstrated the feasibility of using DRIE to fabricate Si photonic crystals for THz frequencies. Stop-bands for TE-polarized light, with transmittance $< 1\%$, were observed from 0.89–1.14 THz and 0.83–1.06 THz for photonic crystals with periods of 100 and 125 μm , respectively.

The authors would like to acknowledge useful discussions with Brian Thibeault. This work was supported by the DARPA QuIST program under Grant No. MDA972-01-1-0027.

¹J. D. Joannopoulos, R. D. Meade, and J. N. Winn, *Photonic Crystals: Molding the Flow of Light* (Princeton University Press, Princeton, NJ, 1995).

²See, for instance, *Mini-Special Issue on Electromagnetic, Crystal Structures, Design, Synthesis, and Applications*, A. Scherer, T. Doll, E. Yablonovitch, H. O. Everitt, and J. A. Higgins, guest editors, IEEE Trans. Microwave Theory Tech. **47**, 2057 (1999).

³See, for instance, *Special Section on Electromagnetic Crystal Structures,*

Design, Synthesis, and Applications, A. Scherer, T. Doll, E. Yablonovitch, H. O. Everitt, and J. A. Higgins, guest editors, J. Lightwave Technol. **17**, 1928 (1999).

⁴E. Ozbay, J. Opt. Soc. Am. B **13**, 1945 (1996).

⁵B. Temelkuran, M. Bayindir, E. Ozbay, J. P. Kavanaugh, M. M. Sigalas, and G. Tuttle, Appl. Phys. Lett. **78**, 264 (2001).

⁶E. Ozbay, E. Michel, G. Tuttle, R. Biswas, M. Sigalas, and K.-M. Ho, Appl. Phys. Lett. **64**, 2059 (1994).

⁷A. Chelnokov, S. Rowson, J.-M. Lourtioz, L. Duvillearet, and J.-L. Coutaz, Electron. Lett. **33**, 1981 (1997).

⁸M. C. Wanke, O. Lehmann, K. Müller, Q. Wen, and M. Stuke, Science **275**, 1284 (1997).

⁹C. Jin, B. Cheng, Z. Li, D. Zhang, L.-M. Li, and Z.-Q. Zhang, Opt. Commun. **166**, 9 (1999).

¹⁰G. Feiertag, W. Ehrfield, H. Freimuth, H. Kolle, H. Lehr, M. Schmidt, M. M. Sigalas, C. M. Soukoulis, G. Kiriakidis, T. Pedersen, J. Kuhl, and W. Koening, Appl. Phys. Lett. **71**, 1441 (1997).

¹¹N. Katsarakis, M. Bender, L. Singleton, G. Kiriakidis, and C. M. Soukoulis, Microsystem Technologies **8**, 74 (2002).

¹²H. Han, H. Park, M. Cho, and J. Kim, Appl. Phys. Lett. **80**, 2634 (2002).

¹³R. Kohler, A. Tredicucci, F. Beltram, H. F. Beere, E. H. Linfield, A. G. Davies, D. A. Ritchie, R. C. Iotti, and F. Rossi, Nature (London) **417**, 156 (2002).

¹⁴Z. Jiang and X.-C. Zhang, Opt. Express **5**, 243 (1999).

¹⁵P.-A. Clerc, L. Dellmann, F. Grétilat, M.-A. Grétilat, P.-F. Indermühle, S. Jeanneret, Ph. Luginbuhl, C. Marxer, T. L. Pfeffer, G.-A. Racine, S. Roth, U. Staufner, C. Stebler, P. Thiébaud, and N. F. de Rooij, J. Micromech. Microeng. **8**, 272 (1998).

¹⁶M. Madou, *Fundamentals of Microfabrication* (CRC Press, Boca Raton, FL, 1997).

¹⁷T. Yoshie, J. Vučković, and A. Scherer, Appl. Phys. Lett. **79**, 4289 (2001).

¹⁸D. Grischkowsky, S. Keiding, M. V. Exter, and Ch. Fattinger, J. Opt. Soc. Am. B **7**, 2006 (1990).

¹⁹W. T. Welford and R. Winston *The Optics of Nonimaging Concentrators: Light and Solar Energy* (Academic, New York, 1978).

²⁰<http://ab-initio.mit.edu/mpb/>

²¹S. G. Johnson and J. D. Joannopoulos, Opt. Express **8**, 173 (2001).